Research on the mechanical property of magnetorheological fluids micro-structure under compression working mode

XINHUA LIU, QINGQING CHEN*, HE LU
School of Mechanical and Electrical Engineering, China University of Mining & Technology, Xuzhou, China

In order to improve the yield stress of magnetorheological fluids, compression working mode of MRF was applied and mechanical property of MRF micro-structure under compression working mode was researched. The form of particles chains was divided into three states and mechanical property of each state was analyzed based on magnetic dipole theory. Analysis results show that the position of particles chains and attached particles play an important role in the mechanical property of MRF micro-structure. Finally, a numerical simulation example was provided and comparison results indicated that the proposed analysis was accurate.

(Received October 17, 2012; accepted April 11, 2013)

Keywords: Magnetorheological fluids, Mechanical property, Compression working mode

1. Introduction

As a kind of prospected function material, magnetorheological fluids (MRF) are composed of micronic magnetic particles with a size of about 10 nm in diameter, carrier liquid and dispersants. When an external magnetic field is applied, MRF would turn the original liquid state to solid state, and this kind of change is rapid, reversible, controllable and proportional to the applied magnetic field [1]. Due to the well rheological properties, MRF have an advantage in developing prospects and engineering applications such as in dampers [2], polishing devices [3], brake actuating system [4-5], even as a possible cancer therapy [6], etc [7-8].

The most important phenomenon of rheological properties shows that suspended particles arrange in a line as a chain in the direction of applied magnetic field. So the working mechanism of MRF chain structure is a necessary research to provide the theoretical foundation for the engineering applications of MRF. The micro-structure of magnetorheological fluids has been an active research area since the last two decades, but at the present stage, the micro-structure researches are almost focusing on that magnetic particles how to form into chains and the micro-structure changes of particles chains under shear mode, and few people research the micro-structure changes of particles chains under compression mode. However the squeeze stress is larger than shear stress, so a better working mechanism for MRF would be proposed through studying on the changes of micro-structure under compression mode and this paper tries to make a detailed research for the problem.

The rest of this paper is organized as follows: some related works are outlined based on literature in section 2. The theoretical basis of chains structure and magnetic dipole is presented in section 3. The detailed process for the analysis of mechanical property is proposed in section 4. A numerical simulation example is provided and the discussion for simulation results is put forward in section 5. The conclusions and future work are summarized in section 6.

2. Literature review

2.1 Research situation of MRF

Recent publications relevant to this paper are mainly concerned with two research streams: one is the simulation approaches of magnetic particles forming into chains and another is the researches and experiments on the working mode of MRF. In this section, we try to summarize the relevant literature.

At present, there are a lot of numerical simulation theories and methods for MRF micro-structure. Sonia [9] et al. analyzed the two-dimensional shape and structure of chain by using molecular dynamics in the rotating magnetic field. Masayuki [10] et al. simulated the two-dimensional micro-structure of magnetorheological fluids using Monte Carlo method. A method of the magnetic particles forming into chain by using Monte Carlo method under three-dimensional area was proposed

[11]. Liu [12] et al. proposed a new simulated method based on cellular element method and Verlet method, and carried out a physics experiment to verify the feasibility and accuracy of dynamic simulation. Zhu [13] et al. established a multi-chain model of MRF based on the view of energy. Liu [14] et al. built a two-phase lattice Boltzmann model to simulate the chainlike structure process of magnetic particles. All these methods prove the accuracy of chain micro-structure of MRF.

Due to the excellent rheological properties of MRF, researches on the experimental study and theory analysis also attracted more and more attention. Zhu [15] et al. established a formula for the calculation of shear stresses founded on Ampere molecular current hypothesis. Truong [16] et al. proposed, designed and fabricated a new model of a linear magnetic actuator that can be applied to the controllable squeeze film damper, and verified to be very effective for attenuation of the vibration of the rotor system by experiment. B. Assadsangabi [17] et al. proposed an optimized design process for a disk-type magneto-rheological brake for automotive applications and proved that braking torque of the present design is larger compared to the previous designs.

Besides, some experimental studies suggested that the yield stress under compression state considerably larger than shear state and the extruding strength of MRF was about one order of magnitude higher than the shear strength [18-19]. Wang [20] et al. raised an experimental method to test compressive and tensile properties, obtained stress-strain curve of compression and showed that the tensile yield stress was about four times of shear yield stress.

2.2 Discussion

Although many simulation methods and experiments of magnetorheological fluids have been developed in above literature, design principle of most MRF devices are based on the shear working mode. Due to the lower yield stress of MRF under shear working mode, usually under 100KPa, it has seriously blocked the development of MRF technology, so a new working mode for MRF should be presented in order to improve the yield stress of magnetorheological fluids.

Nowadays, researches on MRF compression property mostly focus on the experimental observation and analysis [21-22], but the theory study on the mechanical property of magnetorheological fluids micro-structure is poor. Noticeably, it is necessary for the engineering application of MRF to research the micro-mechanism of particles chains compression deformation.

In this paper, the form of particles chains is divided into three states and mechanical property of each state is analyzed based on dipole theory.

3. Theoretical basis

Experiments and theoretical analysis demonstrate that MRF inner particles arrange in the line under an applied magnetic field, and most theoretical models assumed that MRF inner particles arrange end to end. However, not all the particles arrange regularly and there are several particles attaching to the side of absolute straight-sharp particles chains of MRF. According to the main distribution features of attached particles, the form of particles chains can be divided into three states: straight-shaped, satellite-shaped and crossed-shaped, as shown in Fig. 1.

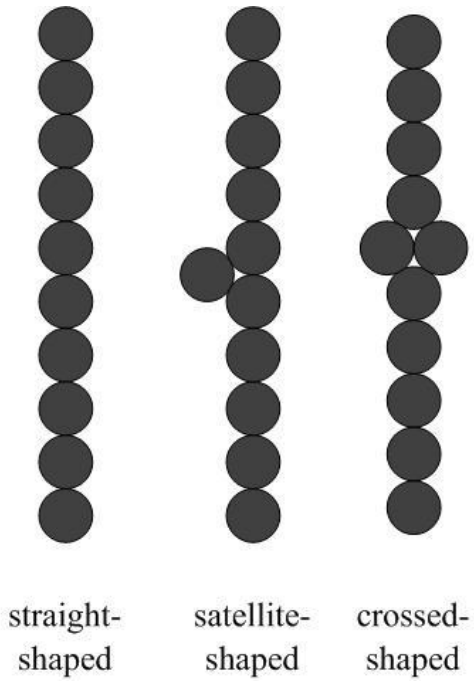

Fig. 1. Three states of attached particles.

According to the theory of magnetic dipole, magnetic force acting on one magnetic particle from another can be expressed as follows [23]:

$$F_i^m = \frac{3\mu_0 m^2}{4\pi r_{ij}^4}\left[\left(1-5\cos^2\theta_{ij}\right)\boldsymbol{r}_{ij}+2\cos\theta_{ij}\boldsymbol{z}\right] \tag{1}$$

Where μ_0 is the permeability of free space, $\boldsymbol{r}_{ij}$ is the relative position vectors between two magnetic particles, θ_{ij} is the angle between $\boldsymbol{r}_{ij}$ and applied magnetic field, $\boldsymbol{z}$ is the unit vectors of magnetic fields and m is the size of magnetic moment. Magnetic moment of magnetic particles in the magnetic field can be calculated as follows:

$$\boldsymbol{m} = \frac{4}{3}\mu_0\mu_1\pi\chi R^3\boldsymbol{H} \tag{2}$$

Where R is the radium of magnetic particle, μ_1 is the relative permeability of carrier liquid, $\boldsymbol{H}$ is the applied magnetic field intensity and χ is the magnetic

susceptibility.

The interaction energy of magnetic dipoles can be expressed as follow [24]:

$$E_{ij} = \frac{1}{4\pi\mu_0\mu_1}\left[\frac{\boldsymbol{m}_i \cdot \boldsymbol{m}_j - 3(\boldsymbol{m}_i \cdot \boldsymbol{e}_r)(\boldsymbol{m}_j \cdot \boldsymbol{e}_r)}{|\boldsymbol{r}|^3}\right] \quad (3)$$

Where $\boldsymbol{m_i}$ is the magnetic moment of particle *i*, $\boldsymbol{m_j}$ is the magnetic moment of particle *j*. $|\boldsymbol{r}|$ is the modulus of $\boldsymbol{r}$ and $\boldsymbol{e}_r$ is the unit vector along $\boldsymbol{r}$.

4. The analysis of mechanical property under compression working mode

Particles arrange into chain-like structures under an applied magnetic field, and the relationship of stress and strain under compression mode is much complicated than other working modes. Because of the incompressibility of MRF and the difference of initial shape and position, MRF will show different mechanical properties under compression mode. Due to the elastic modulus of particles chains is much larger than carrier liquid, particles chains would show the bending deformation in the center part of MRF, but in the edge part of MRF, due to the invariance of volume, the volume of center part is diffused to the edge part, thus, the particles chains would be bended and elongated simultaneously. The following of this paper will discuss the mechanical property of different shaped particles chains under compression mode concretely.

4.1 Mechanical property of straight-shaped particles chain

As shown in Fig. 2a, straight-shaped particles chain would show bending deformation in the center part of MRF. The angle between the line link direction of particles' center and the magnetic direction can be expressed as θ. The center distance between two particles can be expressed as $r=2R$. According to Fig. 2b and formula (1), the formula of force along the direction vertical to the line of centers direction can be derived as follows:

$$F_{mt} = \frac{3\mu_0 m^2}{4\pi(2R)^4}\sin 2\theta \quad (4)$$

The torque caused by magnetic dipole can be derived as follows:

$$M_m = \frac{3\mu_0 m^2}{4\pi(2R)^3}\sin 2\theta \quad (5)$$

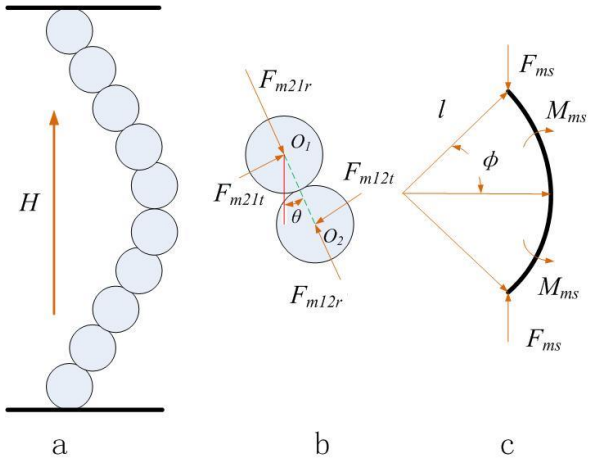

Fig. 2. The schematic diagram of straight-shaped particles chain in the center part of MRF.

Because of the existence of this torque, the angle θ exhibits a decreasing tendency, so we can assume that the torque distributes evenly and continuously. Based on the formula (5), the torque distribution density on the particles chain can be derived as follows:

$$M_{m\rho} = \frac{3\mu_0 m^2}{4\pi(2R)^4}\sin 2\theta \quad (6)$$

Based on the curvature radius l and wrap angle 2ϕ, the counter-balance moment can be derived as follows:

$$\mathrm{M}_{ms} = l\int_0^{\phi}\mathrm{M}_{m\rho}\,d\theta = \frac{3\mu_0 m^2 l}{4\pi(2R)^4}\left(1-\cos^2\phi\right) \quad (7)$$

The torque caused by magneto-compressed force F_{ms} balances with M_{ms}, so F_{ms} can be deduced as follows:

$$F_{ms} = \frac{3\mu_0 m^2 l}{4\pi(2R)^4}(1+\cos\phi) \quad (8)$$

Researches show that in the case of keeping the particles chain's length constant, compression strain ε can be expressed as follows:

$$2\phi l(1-\varepsilon) = 2l\sin\phi \quad (9)$$

So $\phi = \sqrt{6\varepsilon}$, the relationship between magneto-compressed force and compressive strain under pure compression bending can be calculated as follows:

$$F_{ms} = \frac{3\mu_0 m^2 l}{4\pi(2R)^4}\left(1+\cos\sqrt{6\varepsilon}\right) \quad (10)$$

In the edge part of MRF, straight-shaped particles chains would show bended and elongated simultaneously,

as shown in Fig. 3a. The analysis schematic diagram of three adjacent particles is shown in Fig.3b, according to the interaction energy theory and force analysis of magnetic dipole, the force along the centripetal direction of particles chain can be expressed as follows:

$$F_{ci} = 48\pi\mu_0\mu_1 \frac{R^6}{s^4} H^2 \sin\gamma \tag{11}$$

Where γ is the degree of bended, s is the distance of adjacent particles. As shown in Fig. 3 (c), f_{ci} is the distributed force of particles chain and it can be calculated as follows:

$$f_{ci} = \frac{F_{ci}}{s} = 48\pi\mu_0\mu_1 \frac{R^6}{s^5} H^2 \sin\frac{s}{l} \tag{12}$$

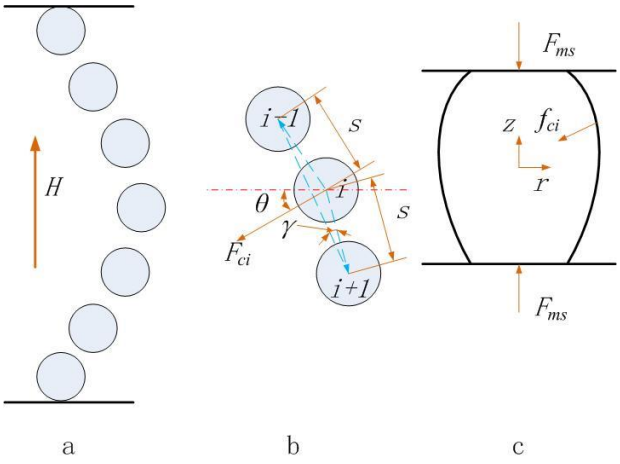

Fig. 3. The analysis schematic diagram of straight-shaped particles chain in the edge part of MRF.

Where l is the curvature radius of particles chain, because of $l \gg s$, $\sin\frac{s}{l} \approx \frac{s}{l}$, so the component expression of F_{ci} along the orientation of z and r can be shown as follows:

$$\begin{cases} F_{cr} = 48\pi\mu_0\mu_1 \dfrac{R^6}{s^4} H^2 \sin\phi \\ F_{cz} = 48\pi\mu_0\mu_1 \dfrac{R^6}{s^4} H^2 (1-\cos\phi) \end{cases} \tag{13}$$

Set $F_{cr} - F_{cz} > 0$, $\phi \in [0\ \pi/2]$, as F_{cr} has an increasing tendency of compression force and F_{cz} is precisely the opposite, so when $\phi < \pi/2$, the combined effect of F_{cr} and F_{cz} makes the compression force increase. Because of the incompressibility of MRF, the compressive deformation along the r direction makes the inner structure more compact and the compressed force will increase inevitably.

4.2 Mechanical property of satellite-shaped particles chain

The shape of satellite-shaped particles chain is shown in Fig. 4a, attached particles and neighboring particles are in triangular permutation, as shown in Fig. 4b. Based on the formula (1), the expression of the resultant force that particle i subjected can be expressed as follows:

$$\begin{cases} F_i^m = 0 \\ F_i^t = \dfrac{3\sqrt{3}\mu_0 m^2}{16\pi(2R)^4} \end{cases} \tag{14}$$

Therefore, attached particle has no influence on the load along the direction of magnetic field and the force along vertical direction of magnetic field makes attached particle have the tendency to move into the chain. The expression of the resultant force of particle j can be expressed as follows:

$$\begin{cases} F_j^m = \dfrac{27\mu_0 m^2}{32\pi(2R)^4} \\ F_j^t = \dfrac{3\sqrt{3}\mu_0 m^2}{32\pi(2R)^4} \end{cases} \tag{15}$$

If particle i doesn't exist, the expression of the resultant force that particle j subjected can be expressed as follows:

$$F_j^{m'} = \frac{3\mu_0 m^2}{2\pi(2R)^4} \tag{16}$$

Thus, due to the existence of attached particle i, the force F_j^m is about half of the force $F_j^{m'}$ and the force F_j^t has the tendency to pull the particle j and k away from particles chain. So it causes the particles chain weakness and the particles chain where the attached particle exists will bend firstly. Therefore, the state of compression deformation is shown in Fig. 4c and the magnitude of F_j^t can be calculated as follows:

$$F_j^t = \frac{3\mu_0 m^2}{4\pi(2R)^4} \left[\sin 2\theta + (1-5\cos^2\theta)\cos\theta\right] \tag{17}$$

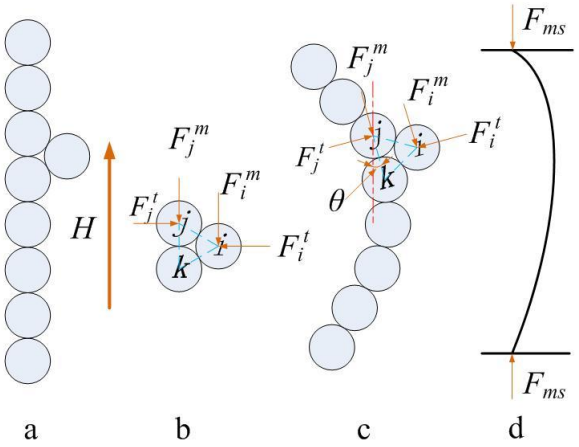

Fig. 4. The schematic diagram of satellite-shaped particles chain in the center part of MRF.

The expression of counter-balance moment M_n can be expressed as follows:

$$M_n = F_j^t \times 2R = \frac{3\mu_0 m^2}{4\pi(2R)^3} \left[\sin 2\theta + (1-5\cos^2\theta)\cos\theta\right] \tag{18}$$

So the torque distribution density on the particles chains can be derived as follows:

$$M_{n\rho} = \frac{3\mu_0 m^2}{4\pi(2R)^4} \left[\sin 2\theta + (1-5\cos^2\theta)\cos\theta\right] \tag{19}$$

Based on the curvature radius l and wrap angle 2ϕ, the counter-balance moment can be derived as follows:

$$M_{ms} = l\int_0^{\phi} M_{m\rho} d\theta = \frac{3\mu_0 m^2 l}{4\pi(2R)^4} \left(1-\frac{1}{2}\cos 2\phi - 4\sin\phi + \frac{5}{3}\sin^3\phi\right) \tag{20}$$

The torque caused by the magneto-compressed force F_{ms} balances with M_{ms} and the force F_{ms} can be deduced as follows:

$$F_{ms} = \frac{3\mu_0 m^2 l}{4\pi(2R)^4} \frac{\left(1-\frac{1}{2}\cos 2\phi - 4\sin\phi + \frac{5}{3}\sin^3\phi\right)}{1-\cos\phi} \tag{21}$$

Since $\phi = \sqrt{6\varepsilon}$, the relationship between magneto-compressed force and compressive strain under pure compression bending can be calculated as follows:

$$F_{ms} = \frac{3\mu_0 m^2 l}{4\pi(2R)^4} \frac{\left(1-\frac{1}{2}\cos 2\sqrt{6\varepsilon} - 4\sin\sqrt{6\varepsilon} + \frac{5}{3}\sin^3\sqrt{6\varepsilon}\right)}{1-\cos\sqrt{6\varepsilon}} \tag{22}$$

In the edge part of MRF, satellite-shaped particles chains would be bended and elongated simultaneously. Due to the force F_i^t has the tendency of pulling the attached particle to the chain, attached particle will be pulled into the chain with the elongating and bending of chain, and the movement tendency of attached particle *i* can be shown as Fig. 5.

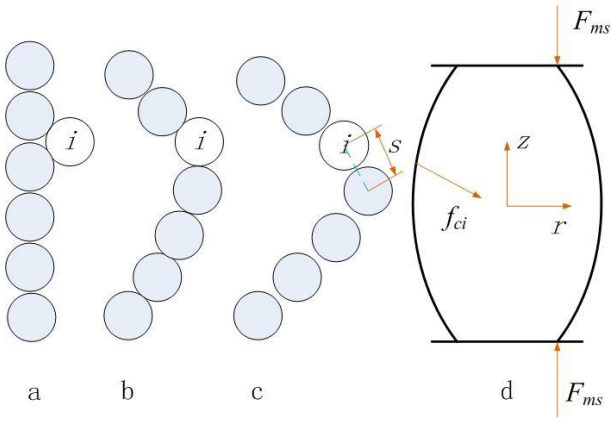

Fig. 5. The schematic diagram of satellite-shaped particles chain in the edge part of MRF.

The satellite-shaped particles chain's change would be the same as the straight-shaped particles chain, so referring to the load status of straight-shaped particles chain, the final form of magneto-compressed force would be similar to the straight-shaped particles chain and the only difference is the delay of time. Thus, the component expression of magneto-compressed force along the

orientation of *z* and *r* can be shown as follows:

$$\begin{cases} F_{cr} = 48\pi\mu_0\mu_1 \dfrac{R^6}{s^4} H^2 \sin\phi \\ F_{cz} = 48\pi\mu_0\mu_1 \dfrac{R^6}{s^4} H^2 \left(1-\cos\phi\right) \end{cases} \tag{23}$$

4.3 Mechanical property of crossed-shaped particles chain

The arrangement of crossed-shaped particles chain is shown in Fig. 6a and the schematic diagram of force analysis is shown in Fig. 6b. Based on formula (1), the expression of resultant force that particle *i* subjected can be expressed as follows:

$$\begin{cases} F_i^m = 0 \\ F_i^t = \dfrac{21\mu_0 m^2}{16\pi\left(2R\right)^4} \end{cases} \tag{24}$$

The expression of resultant force that particle *j* subjected can be expressed as follows:

$$\begin{cases} F_j^m = \dfrac{9\sqrt{3}\mu_0 m^2}{16\pi\left(2R\right)^4} \\ F_j^t = 0 \end{cases} \tag{25}$$

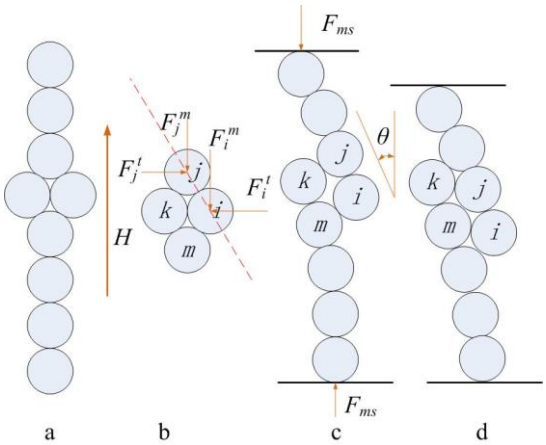

Fig. 6. The schematic diagram of crossed-shaped particles chain in the center part of MRF.

In the center part of MRF, because of the existence of attached particles *i* and *k*, F_j^m is about one third of $F_i^{m'}$, it causes the particles chain weakness on the position where the attached particles exist. The schematic diagram of force analysis and changing tendency is shown in Fig.6b. When deformed under compression, the particles chain would slip in the position of particle *i* and the final form of particles chain is shown in Fig. 6d. The magneto-compressed force F_{ms} can be expressed as follows:

$$F_{ms} = F_j^m \cos\frac{\pi}{6}\cos\theta \tag{26}$$

The tilting angle of particles chain θ is very small, so $\cos\theta \approx 1$. Due to the slip phenomenon of particles chain, the magneto-compressed force F_{ms} can be expressed as follows:

$$F_{ms} = F_j^m \cos\frac{\pi}{6} = \frac{27\mu_0 m^2}{32\pi\left(2R\right)^4} \tag{27}$$

In the edge part of MRF, particles chain will be bended and elongated simultaneously. According to the force analysis of particles *i* and *j*, attached particles have the tendency of moving into the particles chain. With a little of malposition about the particle location, attached particles will be pulled into the particles chain to become straight-shaped particles chain as shown in Fig. 7. The final form of magneto-compressed force will be similar to the straight-shaped particles chain and the only difference is the delay of time. Thus, the component expression of magneto-compressed force along the orientation of *z* and *r* can be shown as follows:

$$\begin{cases} \mathrm{F}_{cr} = 48\pi\mu_0\mu_1 \dfrac{R^6}{s^4} H^2 \sin\phi \\ \mathrm{F}_{cr} = 48\pi\mu_0\mu_1 \dfrac{R^6}{s^4} H^2 \left(1-\cos\phi\right) \end{cases} \tag{28}$$

Where ϕ is the final bending angle of particles chain.

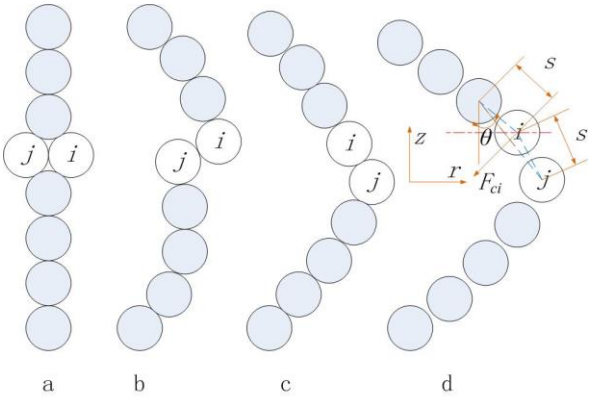

Fig. 7. The change process of crossed-shaped particles chain in the edge part of MRF.

5. Numerical simulation and results discussion

5.1 Flowchart of numerical simulation

Nowadays, due to the advantages of low cost, fast speed and high accuracy, numerical simulation method has been applied as an important and effective solution in the particle fluid system dynamics. There are several simulation methods such as verlet algorithm, velocity-verlet algorithm, shuffled frog-leaping algorithm, predictor corrector algorithm and so on [12]. Velocity-verlet algorithm can provide position, velocity and acceleration simultaneously with high accuracy and this paper uses the velocity-verlet algorithm to simulate the theory analysis. When an external magnetic field is applied, assume the stable micro-structure as shown in Fig. 9(a), the initial velocity of particles is zero and the simulation step is Δt , and the position expression of particles can be expressed as follows:

$$\vec{r}\left(t+\Delta t\right)=\vec{r}\left(t\right)+\vec{v}\Delta t+\frac{1}{2}\vec{a}\left(t\right)\Delta t^2 \quad (29)$$

The velocity expression of particles can be expressed as follows:

$$\vec{v}\left(t+\Delta t\right)=\vec{v}\left(t\right)+\frac{\vec{a}\left(t\right)+\vec{a}\left(t+\Delta t\right)}{2}\Delta t \quad (30)$$

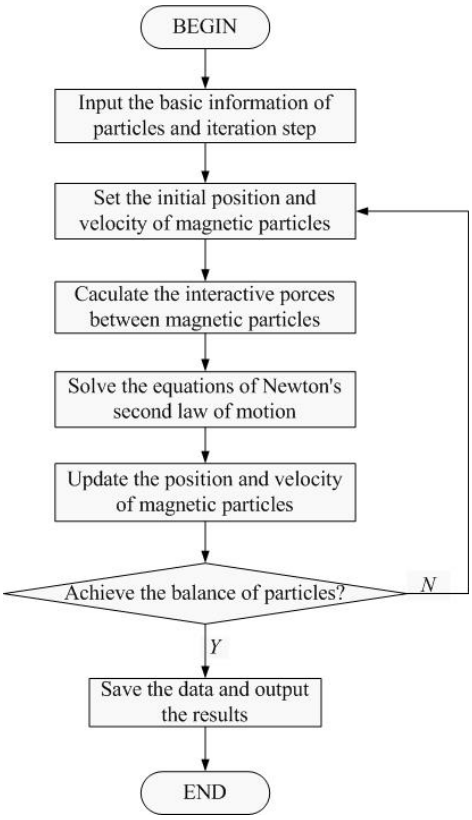

Fig. 8. The flowchart of numerical simulation.

Researches show that the magnetic force F^m , the repulsive force F^r and the viscous resistances of magnetic particles F^v play the major roles in movement process [25], other forces can be ignored. The expressions of repulsive force and viscous resistances of magnetic particles can be expressed as follows:

$$F^r=\sum\nolimits_{j\neq i}\frac{3\mu_0 m^2}{32\pi R^4}\exp\left[-\beta\left(\frac{r_{ij}}{2R}-1\right)\right]\mathrm{r}_{ij} \quad (31)$$

$$F^v=-6\pi R\eta v \quad (32)$$

On the basis of Newton's second law of motion, the kinetic equation of particle motion can be shown as follows:

$$ma=m\frac{d^2r}{dt^2}=F^m+F^r+F^v \quad (33)$$

5.2 Simulation results

In this section, the density of magnetic particles is ρ and the parameters of MRF used in numerical simulation are shown as in Table 1.

Based on the above simulation method and parameters, the simulation results are shown in Fig. 9. The initial state of MRF is shown as Fig. 9a, with the increase of simulation time, the microscopic structure of MRF changes gradually and the motion processes can be shown in Fig. 9a to Fig. 9d.

5.3 Results analysis

As shown in Fig. 9, particles chains are bended in the center part of MRF, while in the edge part of MRF particles chains are bended and elongated simultaneously. Moreover, the attached particles have an influence on the deformation of particles chains. Attached particles will be pulled into the particles chains in the edge part of MRF. While in the center part of MRF, straight-shaped and satellite-shaped particles chains are bended, and the crossed-shaped particles chains are fractured obviously. In brief, the simulation results are same as the theoretical analysis in section 4.

Table 1. The parameters of MRF.

Parameter	β	H(kA /m)	μ_0 (H/m)	χ	η ($pa \cdot s$)	ρ (kg/m^3)	Δt (μs)
Value	9	10	$4\pi\times10^{-7}$	1	0.001	7.9×10^3	20

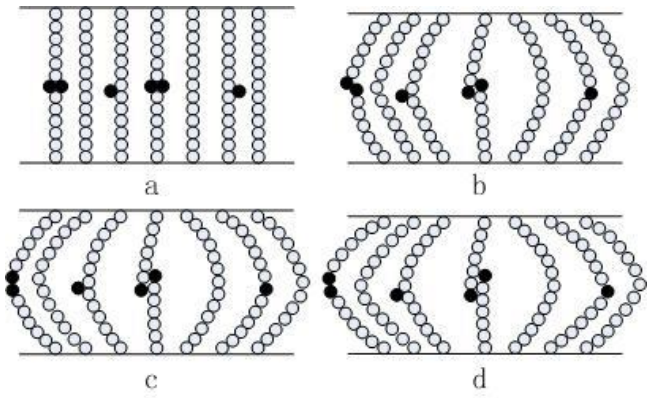

Fig. 9. The simulation results of particles chains under compression mode.

6. Conclusions

In this paper, the mechanical property of MRF particles chains on compression mode was analyzed based on the theory of magnetic particle's dipole model. The analysis results shows that particles chains are bended in the center part of MRF, particles chains are bended and elongated simultaneously in the edge part of MRF. Attached particles have a significant impact on the compressive modulus, in the center part of MRF, straight-shaped and satellite-shaped particles chains are bended, and the presence of cross-shaped attached particles led to the decrease of compressive force obviously. In the edge part of MRF, with the volume squeezing out in the center part of MRF, attached particles are pulled into the particles chains as they are bended simultaneously. The micro-structure of MRF will be more compact during compression process and it increases the concentration of MRF, thus it will improve the compressive modulus.

In this paper, we only focus on the mechanical property of MRF micro-structure under compression working mode and do not consider the influence of saturation magnetization and other factors. In future studies, the authors plan to investigate the mechanical property considering as many as possible factors, and the relationship between compression force and yield stress would also be an important research field for authors.

Acknowledgements

The support of Fundamental Research Funds for the Central Universities (No. 2012QNB14) and the Priority Academic Program Development of Jiangsu Higher Education Institutions in carrying out this research is gratefully acknowledged.

References

[1] X. H. Peng, H. T. Li. Computational Methods in Engineering and Science. Aug, 21, (2006).
[2] Li Junqiang, Zang Xizhe, Zhao Jie, Journal of Mechanical Engineering. **46**(5), 177 (2010).
[3] Sunil Jha & V. K. Jain. International Journal of Advanced Manufacturing Technology. **42**, 656 (2009).
[4] X. H. Liu, Optoelectron. Adv. Mater.-Rapid Commun. **4**(9), 1346 (2010).
[5] A. G. Olabi, A. Grunwald. Materials and Design. **28**, 2658 (2007).
[6] R. Sheng, G. A. Flores, J. Liu. Journal of Magnetism and Magnetic Materials. **194**, 167 (1999).
[7] G. Lacob, A. D. Ciochina, O. Bredetean, M. Racuciu, Optoelectron. Adv. Mater.-Rapid Commun. **2**(7), 446 (2008).
[8] Ajay Sidpara, V. K. Jain. International Journal of Mechanical Sciences. **56**(1), 50 (2012).
[9] Sonia Melle, Oscar G. Calderón, Miguel A. Rubio, Gerald G. Fuller, Journal of Non-Newtonian Fluid Mechanics. **102**(2), 135 (2002).
[10] Masayuki Aoshima, Akira Satoh, Journal of Colloid and Interface Science. **280**, 83 (2004).
[11] Liu Yongzhi, Liu Xinhua, Liu Hao. Procedia Engineering. **15**, 3896 (2011).
[12] Liu Xinhua, Liu Yongzhi, Liu Hao. Advances in Information Sciences and Service Sciences. **4**(12), 55 (2012).
[13] Zhu Ying-shun Gong Xing-long, Li Hui, Zhang Pei-qiang. Journal of China University of Mining & Technology. **35**(4), 498 (2006).
[14] Liu Hao, Liu Xinhua, Liu Yongzhi. Procedia Engineering, **15**, 3948 (2011).
[15] Zhu Changchun, Zhai Pengcheng, Liu Lisheng and Zhang Qingjie, Journal of Wuhan University of Technology. **20**(1), 52 (2005).
[16] Truong Quoc, Thanh, Kyoung Kwan Ahn, Journal of Mechanical Science and Technology. **23**, 344 (2009).
[17] B. Assadsangabi, F. Daneshmand, N. Vahdati, M. Eghtesad, Y. Bazargan-Lari, International Journal of Automotive Technology. **12**(6), 921 (2011).
[18] S. A. Mazlan, A. Issa, H. A. Chowdhury, A. G. Olabi. Materials and Design, **30**, 1985 (2009).
[19] Wang Hong-yun, Gao Chun-pu, Kan Jun-wu, Li Yong-xian, Wang Xiao, Optics and Precision Engineering. **19**(4), 850 (2011).
[20] Wang Hong-yun, Zheng Hui-qiang, Li Yong-xian,

Chinese Journal of Scientific Instrument. **30**(4), 848 (2009).
[21] Yu Tian, Xuli Zhu, Jile Jiang, Yonggang Meng, Shizhu Wen. Smart Materials and Structures. 10(19), 105024 (2010).
[22] S. A. Mazlan, N. B. Ekreem, A. G. Olabi, Journal of Materials Processing Technology. **201**(1-3), 780 (2008).
[23] Li Hai-tao, Peng Xiang-he, Huang Shang-lian, Journal of Functional Materials. **39**(6), 902 (2008).
[24] Zhu Jun-tao, Xu Zhao-dong, Zhang Xiang-cheng, Journal of Southeast University (Natural Science Edition). **41**(2), 342 (2011).
[25] Li Jie-ru, Du Cheng-bin, Journal of Hohai Uifiversity (Natural Sciences). **39**(3), 311 (2011).

*Corresponding author: vrlabpaper@126.com